Autodetachment in H_2^-: A Franck-Condon Approach

Nakul Kushabhau Teke

A dissertation submitted in partial fulfilment of the requirements for the BS-MS dual degree in Chemical Sciences

Indian Institute of Science Education and Research Mohali

April 2016

Certificate of Examination

This is to certify that the dissertation titled "**Autodetachment in H_2^-: A Franck-Condon Approach**" submitted by **Mr. Nakul Kushabhau Teke** (Reg. No. MS11055) in partial fulfilment of the requirements for the BS-MS dual degree of the Institute, has been examined by the thesis committee duly appointed by the Institute. The committee finds the work done by the candidate satisfactory and recommends that the report be accepted.

Dr. K. R. Shamasundar Dr. P. Balanarayan Professor N. Sathyamurthy (Supervisor)

Dated: April 22, 2016

Declaration

The work presented in this dissertation has been carried out by me under the guidance of Professor N. Sathyamurthy at the Indian Institute of Science Education and Research Mohali.

This work has not been submitted in part or in full for a degree, a diploma, or a fellowship to any other university or institute. Whenever contributions of others are involved, every effort is made to indicate this clearly, with due acknowledgement of collaborative research and discussions. This thesis is a bonafide record of original work done by me and all sources listed within have been detailed in the bibliography.

Nakul Kushabhau Teke

(Candidate)

Dated: April 22, 2016

In my capacity as the supervisor of the candidate's project work, I certify that the above statements by the candidate are true to the best of my knowledge.

Professor N. Sathyamurthy

(Supervisor)

विद्वत्वं च नृपत्वं च नैव तुल्यं कदाचन ।
स्वदेशे पूज्यते राजा विद्वान् सर्वत्र पूज्यते ॥

Scholarship and kingship can never be equated.

A king is respected in his own kingdom whereas a scholar is respected everywhere.

- Chanakya (371 BC- 283 BC)

Acknowledgement

I am grateful to...

Professor N. Sathyamurthy for his proficient guidance of my masters' project.

All my gurus, present and past, for their faith in me and their teaching that made me what I am.

My parents Lalita and Kushabhau Teke, my sister Manali for their continous support and encouragement.

Prof. R. J. LeRoy (University of Waterloo) and Dr. Saurabh Srivastava (NIMS, Japan) for their technical help.

Computing facility, IISER Mohali for their prompt services.

...my friends: without you, I could not have done this any better!

Nakul Teke

IISER Mohali

List of Figures

3.1 Potential energy curves of different states of H_2^- and H_2 . The excited states of H_2 are plotted from the work of Barca *et al.* 15

3.2 Effective potentials of H_2 plotted for different values of the rotational quantum number J 16

3.3 Effective potentials of H_2^- plotted for different values of the rotational quantum number J 16

3.4 RPC plotted from the analytic PEC of H_2^- and H_2 17

3.5 Bound states of H_2^- and H_2 calculated for J= 0. 17

3.6 Bound states of H_2^- and H_2 calculated for J= 5 and 10. 18

3.7 Bound states of H_2^- and H_2 calculated for J= 15 and 20. 19

3.8 Bound states of H_2^- and H_2 calculated for J= 25 and 26. 20

3.9 Bound states of H_2^- and H_2 calculated for J= 27 and 28. 21

3.10 Bound states of H_2^- and H_2 calculated for J= 29 and 30. 22

3.11 Franck-Condon Factors calculated between all vibrational states of J=26 of H_2^- and H_2 23

3.12 The photodetachment cross section of H_2^- plotted as a function of photon energy. 23

List of Tables

4.1 Vib-rotational levels of H_2^- in eV units, computed in present work. . . . 26
4.2 Vib-rotational levels of H_2 in eV units, computed in present work. . . . 27

Acronyms

AD	Associative detachment
HF	Hartree-Fock
FCI	Full Configuration Interaction
CBS	Complete Basis Set
EOM	Equation-of-Motion
EOM-CC	Equation-of-Motion Coupled Cluster
PEC	Potential Energy Curve
RPC	Reduced Potential Energy Curve

Contents

List of Figures **v**

List of Tables **vii**

Acronyms **viii**

Abstract **xi**

1 Introduction **1**

1.1 The hydrogen molecular anion H_2^- 1

1.2 Open-shell species 2

2 Methods **5**

2.1 The one-dimensional Schrödinger equation 5

2.2 The Born-Oppenheimer approximation 6

2.3 Reduced potential-energy curve (RPC) 7

2.4 Bound states 7

2.5 Franck-Condon factors 9

2.6 Equation-of-motion coupled-cluster (EOM-CC) formalism 9

2.7 Dyson orbitals 10

2.8 Description of the ejected electron 10

2.9 Cross-section calculation 11

2.9.1 The photodetachment cross section 11

2.9.2 Oscillations in the photodetachment spectrum of H_2^- 12

3 Results and Discussion **13**

3.1 Potential-energy curves for H_2^- and H_2 13

3.2 Effective potential 13

3.3 Reduced potential energy curve 14

3.4 Bound state calculations 14

3.5 Franck-Condon factors 14

3.6 Photodetachment cross section 14

3.7 Outlook 15

4 Appendix **25**

Bibliography **28**

Abstract

Effective potentials are calculated for different values of J, the rotational angular momentum quantum number, from accurate potential energy curves of the $X^2\Sigma_u^+$ state of the molecular hydrogen anion (H_2^-). The bound states of these effective potentials are determined numerically. Autodetachment in H_2^- is studied from a Franck-Condon perspective. The states with maximum probability of transition from H_2^- to H_2 are identified. The photodetachment cross section of H_2^- is calculated as a function of photon energy.

Chapter 1

Introduction

This work is focused on studying autodetachment in H_2^- from a Franck-Condon point of view. The hydrogen molecular anion H_2^- is perhaps the smallest molecular anion. This chapter reflects on the available literature on H_2^- and the relevance of this problem. Chapter 2 focuses on the theoretical aspects of the problem and methods. The results are discussed in Chapter 3.

1.1 The hydrogen molecular anion H_2^-

The hydrogen molecular anion (H_2^-) is perhaps the simplest molecular anion with two nuclei and three electrons. It is thought to play an important role in the formation of molecular hydrogen in the universe. In the associative detachment (AD) of H and H^-, H_2^- acts as an intermediate : $H^- + H \longrightarrow H_2^- \longrightarrow H_2 + e^-$. H_2^- was encountered for the first time experimentally by Khovestenko and Dukel'skii using mass spectrometry[1] in 1958 and later by Hurley[2] in 1974. Aberth *et al.* confirmed the isotopes detecting HD^- and D_2^- in 1975. Experiments and theories have proven to be inadequate in explaining the energy dependence of rate coefficients in AD.[3,4] Rather than being an unstable transient species, the existence of metastable states of H_2^- manifests its stability towards autodetachment and spontaneous dissociation.[5] In recent studies, these states are found to be stable in higher angular momentum. H_2^-

and D_2^- were proved to be existent experimentally by Golser *et al.*[6] Lifetimes of the three isotopologs of the molecular hydrogen anion were measured using electrostatic ion-beam trap by Heber *et al.*[7] and the long lived states of H_2^- were investigated within the non-local resonance model by Čížek *et al.*[8]

The electronic structure calculations of the potential energy curve (PEC) of the excited states of H_2^- calculated using the MRCI method results in variational collapse.[9] This results in a wavefunction comprising a neutral molecule and a free electron (NMFE) state. In this direction, Srivastava *et al.* calculated accurate PEC for the $X^2\Sigma_u^+$ state of H_2^-.[10] They concluded that, at a Full CI level, the correlation-consistent basis sets are the best possible to obtain the complete basis set (CBS) limit for this system. Diffuse basis functions like the augmented basis sets result in variational collapse. They fitted an analytical function to the accurate CBS potential, calculated the vibrational bound states and compared them with those of the ground electronic state of H_2.

1.2 Open-shell species

Molecules are formed by attraction between atoms forming a chemical bond. A chemical bond is formed from electronic interaction (ionic bond) or by sharing of electrons (covalent bond). Homolytic cleavage of covalent bonds leads to the formation of radicals. Open-shell species are atoms or molecules with one or more unpaired electrons.

Open-shell species are transient intermediates in many chemical reactions. It is essential to understand the electronic structure of open-shell species to discern mechanisms of reactions. These reactions are observed in processes like photosynthesis, vision, drug activity, aging process, enzyme catalysis, combustion, atmospheric chemistry, astrochemistry, etc.

Extensive studies of organic, inorganic, metal-organic, and cluster anions have bolstered the field of anion spectroscopy. Photodetachment experiments help in determining structures of unstable and excited states, in ultrafast dynamics, anion reactivity and intermolecular interactions.

Photoelectron spectroscopy can provide an insight into the electronic structure of molecules and ions, and their interaction with light. A measurement of kinetic energy of ejected electrons gives information on the electronic and vibrational levels of ionized molecules, which are dependent on the potential energy surfaces (PESs) of species involved. Information about initial and final state electronic wave functions can be determined by measuring the angular distribution of photoelectrons.

Chapter 2

Methods

This chapter provides an introduction to basic concepts and theory. The one-dimensional Schrödinger equation, Born-Oppenheimer approximation, Franck-Condon Factors, Equation-of-Motion Coupled Cluster Formalism, Dyson orbitals and Scattering cross-section are discussed.

2.1 The one-dimensional Schrödinger equation

The nuclear motion of diatomic molecules is described within Born-Oppenheimer approximation (discussed in section 2.2). The radial one-dimensional Schrödinger equation for a diatomic system is given by[11] :

$$-\frac{\hbar^2}{2\mu}\frac{d^2\Psi_{v,J}}{dr^2} + V_{eff}(r)\Psi_{v,J}(r) = E_{v,J}\Psi_{v,J}(r), \tag{2.1}$$

where

$$V_{eff}(r) = V(r) + J(J+1)\frac{\hbar^2}{2\mu r^2}$$

In this equation, $\hbar$ is Planck's constant divided by 2π, μ is the redued mass of the diatomic system, J is the rotational quantum number and r is the distance between the nuclei. The effective one-dimensional potential is the sum of the centrifugal term and rotationless elecrtonic potential *V(r)*.

2.2 The Born-Oppenheimer approximation

The Born-Oppenheimer approximation is used for finding approximate solutions of the time-independent non-relativistic Schrödinger equation: $\mathcal{H}|\Phi\rangle = \mathcal{E}|\Phi\rangle$. The Hamiltonian $\mathcal{H}$ for a system of M nuclei and N electrons is given by:[12]

$$\mathcal{H} = -\sum_{i=1}^{N} \frac{1}{2}\nabla_i^2 - \sum_{A=1}^{M} \frac{1}{2M_A}\nabla_A^2 - \sum_{i=1}^{N}\sum_{A=1}^{M} \frac{Z_A}{r_{iA}} + \sum_{i=1}^{N}\sum_{j>i}^{N} \frac{1}{r_{ij}} + \sum_{A=1}^{M}\sum_{B>A}^{M} \frac{Z_A Z_B}{R_{AB}} \quad (2.2)$$

The nuclei in an atom or a molecule are heavier than electrons; hence they move slowly relative to the electrons. It is a reasonable approximation to consider the electrons moving in a field of fixed nuclear configuration. Within the Born-Oppenheimer approximation, the kinetic energy of nuclear motion (second term in eq. 2.2 can be neglected and the nuclear-nuclear repulsion can be considered constant. The modified equation is a Hamiltonian describing the motion of N electrons in the field of M point charges. This is called the electronic Hamiltonian. It is given by:

$$\mathcal{H}_{ele} = -\sum_{i=1}^{N} \frac{1}{2}\nabla_i^2 - \sum_{i=1}^{N}\sum_{A=1}^{M} \frac{Z_A}{r_{iA}} + \sum_{i=1}^{N}\sum_{j>i}^{N} \frac{1}{r_{ij}} \quad (2.3)$$

The solution to the electronic Hamiltonian is the electronic wave function given by Φ_{ele}, which describes the electronic motion.

$$\Phi_{ele} = \Phi_{ele}(\mathbf{R_i}; \mathbf{R_A})$$

Φ_{ele} is explicitly dependent on electronic coordinates. Also, Φ_{ele} and $\mathcal{E}_{ele}$ depend parametrically on nuclear coordinates. The total energy $\mathcal{E}_{tot}$ includes the constant repulsion between the nuclei.

$$\mathcal{E}_{tot} = \mathcal{E}_{ele} + \sum_{A=1}^{M}\sum_{B>A}^{M} \frac{Z_A Z_B}{R_{AB}} \quad (2.4)$$

The motion of the nuclei can be studied by invoking the Born-Oppenheimer approximation. The electrons are lighter than the nuclei, hence they move faster than the nuclei. This can be used to average the electronic co-ordinates and generate a nuclear

Hamiltonian for the motion of the nuclei in the average field of electrons.

$$\mathcal{H}_{nuc} = \sum_{A=1}^{M} \frac{1}{2M_A} \nabla_A^2 + \mathcal{E}_{ele} + \sum_{A=1}^{M} \sum_{B>A}^{M} \frac{Z_A Z_B}{R_{AB}} \tag{2.5}$$

$$\mathcal{H}_{nuc} = \sum_{A=1}^{M} \frac{1}{2M_A} \nabla_A^2 + \mathcal{E}_{tot} \tag{2.6}$$

Thus, the potential for nuclear motion is provided by the total energy $\mathcal{E}_{tot}$. To conclude, within the Born-Oppenheimer approximation, the nuclei move on a surface generated by solving the electronic problem.

2.3 Reduced potential-energy curve (RPC)

Potential energy curves of a diatomic molecule and its cation are nearly identical in reduced variables.[13] This is a manifestation of the fact that the force constant in reduced variables is nearly the same for a diatomic molecule and its cation.

2.4 Bound states

Bound states of diatomic species can be calculated from the potential energy curves using the *Numerov mothod*[14]. Equation 2.1 is an eigenvalue problem and we find the solutions that vanish at $r = \pm\infty$. A suitable method for solving such an equation is the *Numerov method*. The method for calculating eigenvalues and corresponding eigenfunctions and its implemnetation is presented by Cooley.[14] The Schrödinger equation can be written as a second order equation that is linear in ψ and does not have a first order term,

$$\frac{d^2\psi(x)}{dx^2} + k^2(x)\psi(x) = 0 \tag{2.7}$$

In the *Numerov method*, $\psi(x+h)$ is expanded in a Taylor series:

$$\psi(x+h) = \psi(x) + h\psi'(x) + \frac{h^2}{2}\psi^{(2)}(x) + \frac{h^3}{6}\psi^{(3)}(x) + \frac{h^4}{24}\psi^{(4)}(x) + ... \tag{2.8}$$

Similarly, the Taylor expansion of $\psi(x-h)$ gives:

$$\psi(x-h) = \psi(x) - h\psi'(x) + \frac{h^2}{2}\psi^{(2)}(x) - \frac{h^3}{6}\psi^{(3)}(x) + \frac{h^4}{24}\psi^{(4)}(x) + ... \tag{2.9}$$

Adding these two equations 2.8 and 2.9, we obtain

$$\psi(x+h) + \psi(x-h) = 2\psi(x) + h^2\psi^{(2)}(x) + \frac{h^4}{12}\psi^{(4)}(x) + ... \tag{2.10}$$

The second derivative from Equation 2.7 can be written as:

$$\psi^{(2)}(x) = \frac{\psi(x+h) + \psi(x-h) - 2\psi(x)}{h^2} - \frac{h^2}{12}\psi^{(4)}(x) + ... \tag{2.11}$$

Acting $1 + \frac{h^2}{12}\frac{d^2}{dx^2}$ on Equation 2.7 gives:

$$\psi^{(2)}(x) + \frac{h^2}{12}\psi^{(4)}(x) + k^2(x)\psi(x) + \frac{h^2}{12}\frac{d^2}{dx^2}[k^2(x)\psi(x)] = 0 \tag{2.12}$$

From Equations 2.11 and 2.12, we obtain

$$\psi(x+h) + \psi(x-h) - 2\psi(x) + h^2k^2(x)\psi(x)\frac{h^4}{12}\frac{d^2}{dx^2}[k^2(x)\psi(x)] = 0 \tag{2.13}$$

Using elementary difference formula:

$$\frac{d^2}{dx^2}[k^2(x)\psi(x)] \simeq \frac{k^2(x+h)\psi(x+h) + k^2(x-h)\psi(x-h) - 2k^2(x)\psi(x)}{h^2} \tag{2.14}$$

Substituting Eq. 2.14 into 2.13, the Numerov algorithm for a single step is obtained:

$$\psi(x+h) = \frac{2(1 - \frac{5}{12}h^2k^2(x))\psi(x) - (1 + \frac{1}{12}h^2k^2(x-h))\psi(x-h)}{1 + \frac{1}{12}h^2k^2(x+h)} \tag{2.15}$$

Now, we set $x = x_n \equiv x_0 + nh$ and $k_n \equiv k(x_n)$, and the final result is:

$$\boxed{\psi_{n+1} = \frac{2(1 - \frac{5}{12}h^2k_n^2)\psi_n - (1 + \frac{1}{12}h^2k_{n-1}^2)\psi_{n-1}}{1 + \frac{1}{12}h^2k_{n+1}^2}} \tag{2.16}$$

Thus, given ψ_0 and ψ_1, ψ_n can be determined for $n = 2, 3, 4, 5, ...$ using the Numerov method. [15]

2.5 Franck-Condon factors

Franck-Condon factor is an overlap integral between the wave functions for the vibrotational states of the ground electronic state and an excited electronic state. They are given by:

$$| \langle \Psi_{v',J'} | \Psi_{v'',J''} \rangle |^2$$

The electronic transitions occur on shorter time scales compared to the nuclear motion. This is called the Condon approximation.

2.6 Equation-of-motion coupled-cluster (EOM-CC) formalism

Theoretical modelling of open-shell and electronically excited species is challenging because of electronic degeneracies resulting in interacting electronic states and multi-configurational wave functions. Thus, the Hartree-Fock method fails and the ground-state methods that describe the wave function as a single Slater determinant become inadequate. With EOM, many multi-configurational wave functions can be described within the single reference formalism. EOM-CC methods can be used to describe ionization from open-shell species and electronically excited states.[16] Formal aspects of the theory and application of the EOM-CC method to open-shell ground and excited electronic states is reviewed by Krylov.[17]

The EOM approach is analogous to the configuration interaction (CI) method. Diagonalization of the similarity transformed Hamiltonian yields target EOM states. The similarity transformed Hamiltonian $\bar{H}$ is

$$\bar{H} \equiv e^{-T} H e^{T},$$

where T is a cluster operator given by:

$$T = T_1 + T_2 + T_3 + ...$$

with $T_1 = \sum_i \sum_a t_a^i a^+ i$ and $T_2 = \sum_{i,j} \sum_{a,b} t_{ab}^{ij} a^+ b^+ ji$. Also,

$$\bar{H}R = ER$$

$$L\bar{H} = EL$$

$$L_I R_J = \delta_{IJ}$$

Here, R and L are excitation and de-excitation operators, respectively, with respect to the reference $|\Psi_\circ\rangle$. These operators are not electron conserving in case of electron detached/attached EOM models giving rise to EOM-ionization potential (IP) or EOM-electron affinity (EA) models. For instance, R in EOM-IP is given by:

$$R^{IP} = \sum_i r_i i + \frac{1}{2}\sum_{ija} r^a_{ij} a^+ ji + ...,$$

where $a^+$is a creation operator and j and i are annihilation operators. Unlike single reference methods, EOM-IP yields accurate PESs, diabatic couplings for charge-transfer processes and explains charge localization.

2.7 Dyson orbitals

Dyson orbitals describe the overlap between the N-electron wave function of the neutral and the N-1 electron wave function of the corresponding ionized system. They are required for calculating Compton profiles, electron momentum spectra, cross sections and angular distribution of photoelectrons during photodetachment. Dyson orbitals are implemented for equation-of-motion coupled-cluster wave function by Oana and Krylov.[18]

2.8 Description of the ejected electron

The ejected electrons are described using a simple plane wave in spherical basis. In the absence of interaction between the core and the ejected electron, the plane wave is an exact eigenstate of a free electron. The interaction is neglected since the core is small relative to continuous states of the electron. If photodetachment results in a neutral core (in the case of anions), there is no long range Coulombic potential.

For a correct threshold behaviour, a strong orthogonality condition is imposed making the plane wave orthogonal to the Dyson orbital. The expression for a free electron is given by:

$$\Psi_k^{el} = |k\rangle = \left(\frac{k}{(2\pi)^3}\right)^{\frac{1}{2}} e^{ikr}$$

2.9 Cross-section calculation

2.9.1 The photodetachment cross section

The differential cross section for ionizing or detaching a photoelectron in a solid angle $d\Omega_k = sin\theta d\theta d\phi$ is

$$\frac{d\sigma}{d\Omega_k} = \frac{4\pi^2}{c} E |D_k^{IF}(\theta, \phi)|^2$$

where E is the energy of the ionizing radiation, $\boldsymbol{k}$ denotes the momentum and the direction of the ejected electron, D_k^{IF} is the photoelectron matrix element. This is valid within dipole and sudden ionization approximations. A strong orthogonality condition is also imposed to ensure no interaction between the ejected electron and the electron core. These approximations are justified by the small core size relative to the free electron wave function.

For molecular systems, vibrational wave functions of initial and final states are included in dipole matrix element and the above equation becomes:

$$\frac{d\sigma}{d\Omega_k} = \frac{4\pi^2}{c} E \sum_{nn'} P_n |D_{nn'k}|^2$$

where n and n' describe initial and final vibrational levels and P_n denotes the population of the vibrational states of the initial system. $D_{nn'k}$ includes contributions from electronic and vibrational wave functions. The dependence of the electronic dipole matrix element on nuclear coordinates is neglected within the Condon approximation. On averaging over all molecular orientations, we obtain

$$\frac{d\sigma}{d\Omega_k} = \frac{4\pi^2}{c} E \overline{|D_{nn'k}|^2}$$

The total cross section (σ) after averaging over laser polarization and orientation of photoelectrons is obtained from

$$\sigma = \frac{8\pi^2}{3c} E \int d\Omega_k \overline{|D_k^{IF}|^2} = \frac{8\pi^2}{3c} E \int \sin(\theta) d\theta d\phi \overline{|D^{IF}(\theta, \phi)|^2}$$

2.9.2 Oscillations in the photodetachment spectrum of H_2^-

The experimental measurement of the photodetachment cross section of H_2^- was performed by Rudnev *et al.*[19] The same group reported the first experimental photodetachment cross section spectrum of H_2^-.[20] They calculated the absolute cross section in the laser excitation range $E_{h\nu}$= 17600-17750 cm^{-1} (2.1820 - 2.2007 eV). The cross section exhibited an oscillatory behaviour with a period of about 25 cm^{-1}. They fitted a cosine function to the data points. They interpreted the oscillatory behaviour in terms of the interaction between rotationally hot hydrogen molecule and the detached electron after photodetachment.

Chapter 3

Results and Discussion

This chapter comprises results obtained from all the calculations. The effective potentials for H_2 and H_2^- are plotted as a function of internuclear distance. The reduced potential energy curves (RPC) are also plotted. The results from bound state calculation and Franck-Condon factors are discussed.

3.1 Potential-energy curves for H_2^- and H_2

The potential energy curves (PECs) for H_2 and H_2^- were calculated using the MOLPRO suite of programs. The resulting *ab iniitio* data were reproduced using the analytic function by Srivastava *et al.*[10] The PECs for the excited states of H_2 ($b^3\Sigma_u^+$ and $B^1\Sigma_u^+$) are from Barca *et al.*[21] The plots are shown in Figure 3.1.
For photo-excitation of H_2^- , Rudnev *et al.* used light with a wavelength of 563 - 568 nm (2.20216 - 2.18277 eV).[20] The $B^1\Sigma_u^+$ state of H_2 is higher in energy than where the light with a wavelength of 563 - 568 nm can take H_2^- . Therefore, it is safe to assume that the $B^1\Sigma_u^+$ state of H_2 has no role to play in the photodetachment of H_2^- .

3.2 Effective potential

Effective potentials were calculated for J ranging from 0 to 30 of H_2^- and H_2 . Figure 3.2 and Figure 3.3 show the PECs for H_2 and H_2^- , respectively for different values of

J. These curves were used to calculate the bound and quasi-bound states and their line widths.

3.3 Reduced potential energy curve

The reduced potential energy curves (RPC) are plotted for H_2^- and H_2 on the same plot in Figure 3.4. Contrary to the observations of Abrol *et al.*,[13] the RPCs of the neutral (H_2) and its anion (H_2^-) are significantly different.

3.4 Bound state calculations

Using the effective potentials generated as mentioned in section 3.1, the bound states of H_2 and H_2^- were calculated using the computer code LEVEL8.2.[11] The number of bound states of both H_2 and H_2^- decrease with an increase in J value. The number of bound states for all effective potentials and their energy eigenvalues are given in tables 4.2 and 4.1 for H_2 and H_2^- , respectively.

3.5 Franck-Condon factors

The Franck-Condon Factors (FCFs) for the transition between different vibrational levels of J= 26 of H_2^- to J= 26 of H_2 are plotted in Figure 3.11. From the plot, it can be seen that the transition between the lowest level of H_2^- ($v' = 0$) to the highest level of H_2 (v" $= 5$) is the strongest.

3.6 Photodetachment cross section

The total cross section of photodetachment of H_2^- as a function of photon energy was calculated using the *ezDyson* program.[22] *ezDyson* is a C++ program that calculates the absolute photodetachment cross sections using Dyson orbitals computed by an *ab initio* program. The result is plotted in Figure 3.12.

3.7 Outlook

While calculating the photodetachment cross section, a strong orthogonality condition is imposed between the wave function of the ejected electron and the daughter molecule. This is a bold assumption ignoring the *J*-*S* coupling that might result in the oscillatory behaviour in the photodetachment spectrum. *J*-*S* coupling needs to be accounted for while calculating the cross-section.

Moreover, long range interaction needs to be studied for H_2^- . The co-efficient of r^{-4} term in the analytic function used to fit the *ab initio* data of H_2^- is absent. This co-efficient accounts for the charge - polarizability interaction in the potential and thus needs to be accounted for.

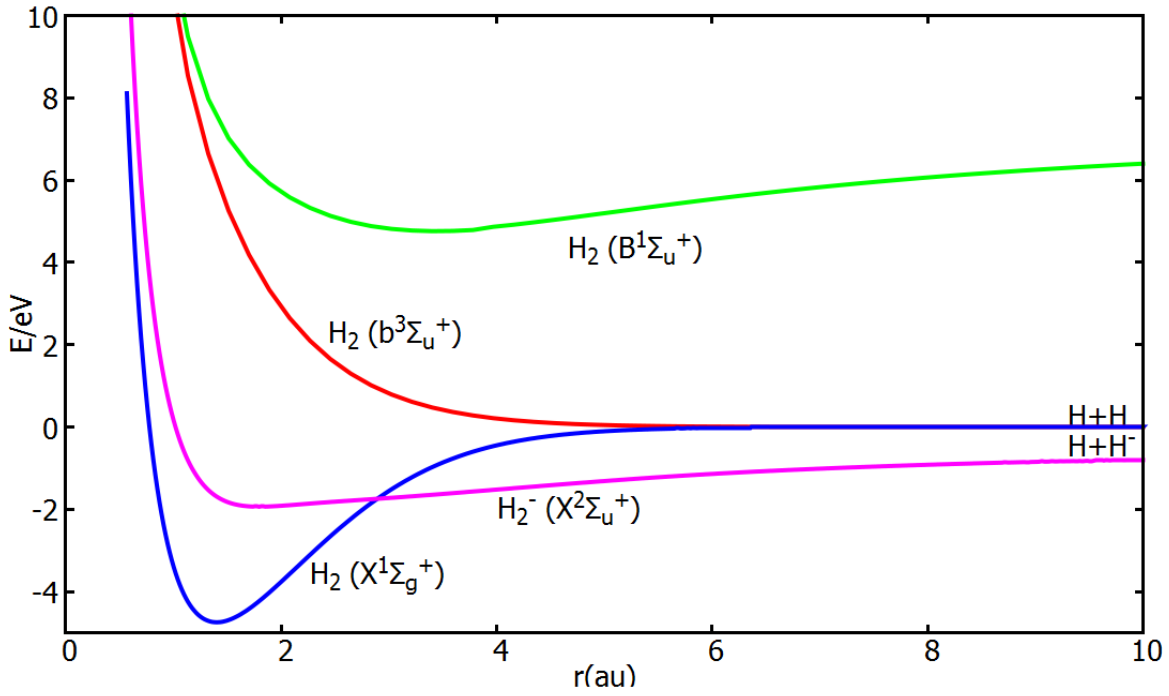

Figure 3.1: Potential energy curves of different states of H_2^- and H_2 . The excited states of H_2 are plotted from the work of Barca *et al.*

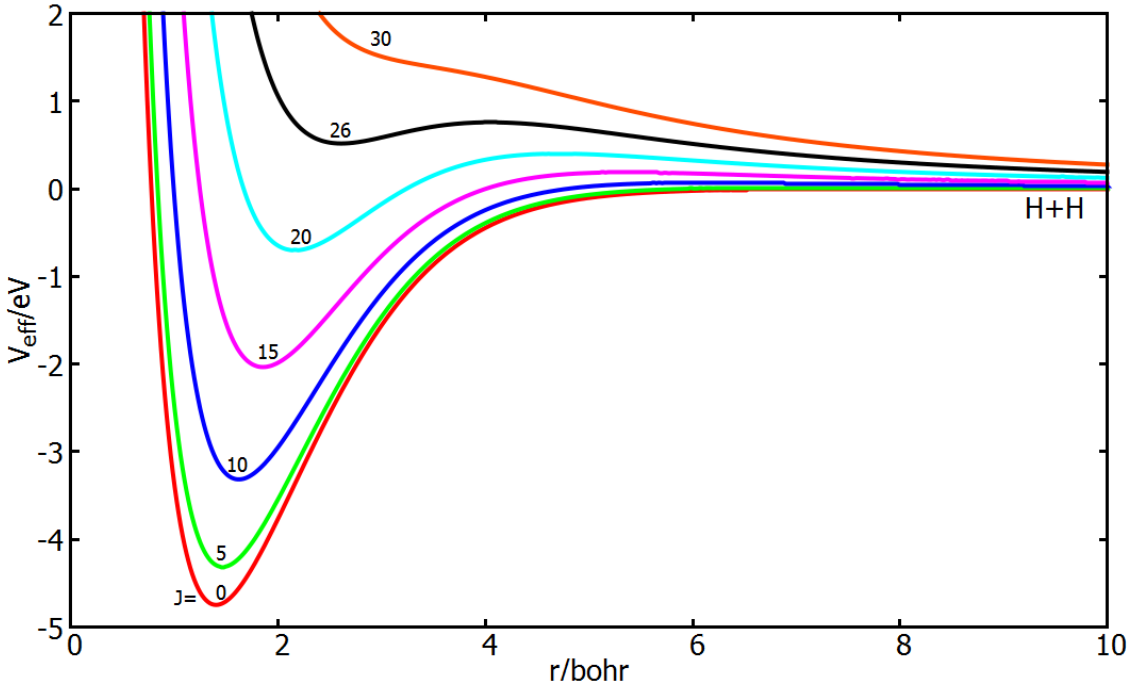

Figure 3.2: Effective potentials of H_2 plotted for different values of the rotational quantum number J

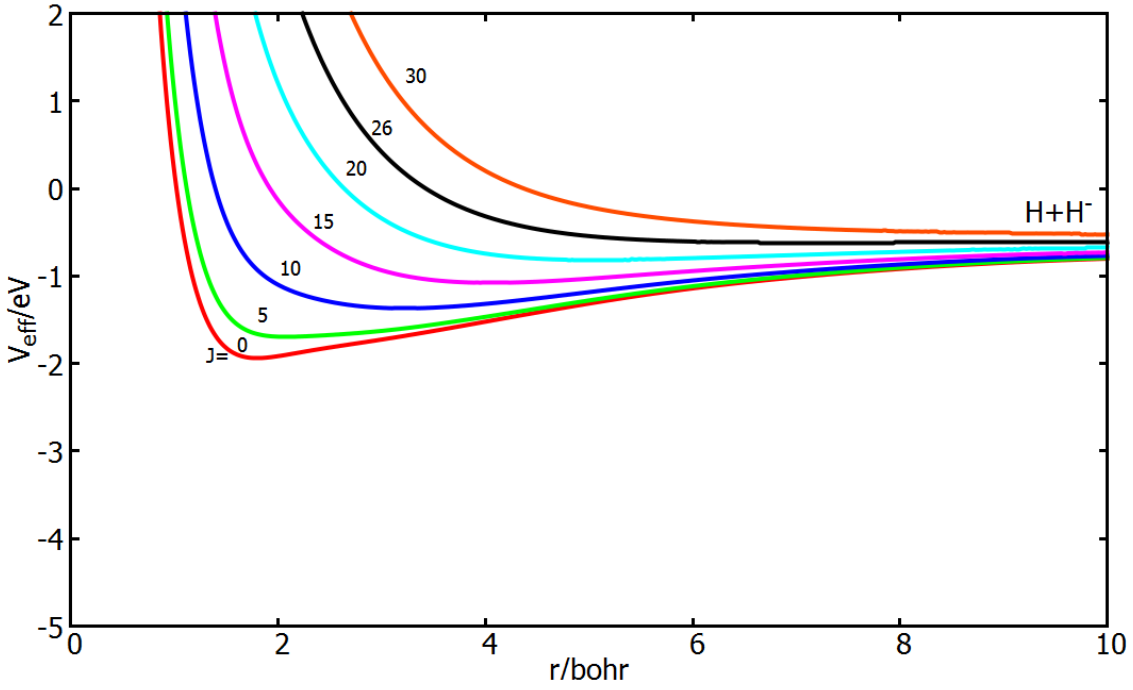

Figure 3.3: Effective potentials of H_2^- plotted for different values of the rotational quantum number J

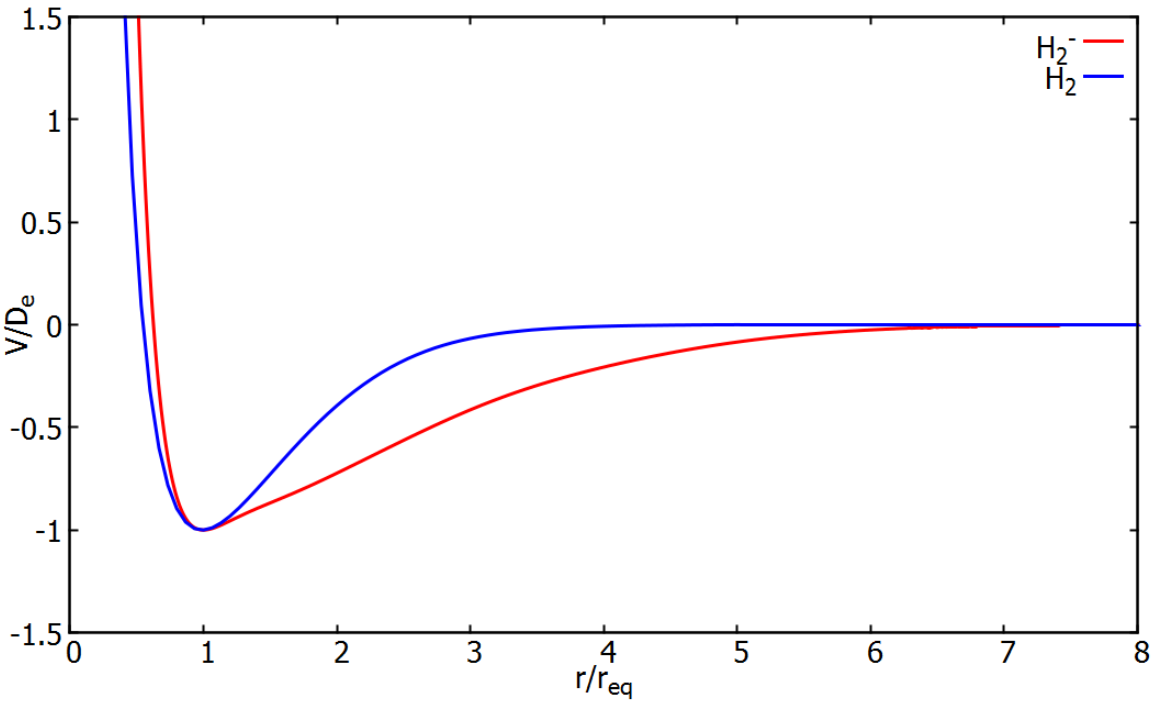

Figure 3.4: RPC plotted from the analytic PEC of H_2^- and H_2

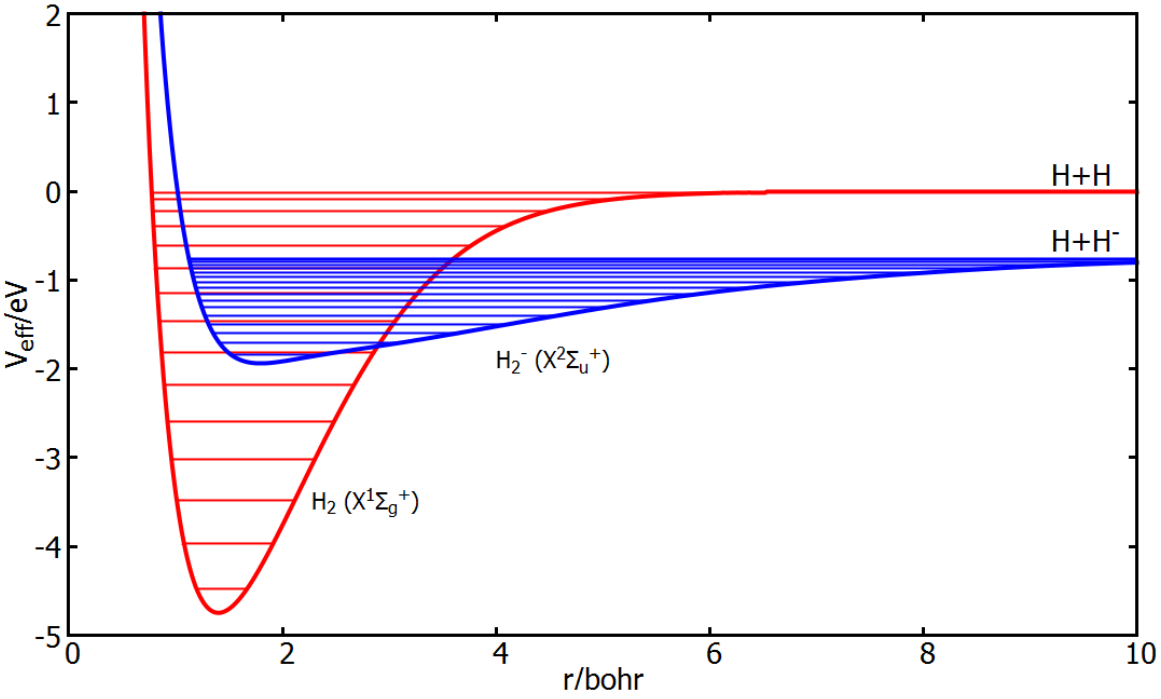

Figure 3.5: Bound states of H_2^- and H_2 calculated for $J = 0$.

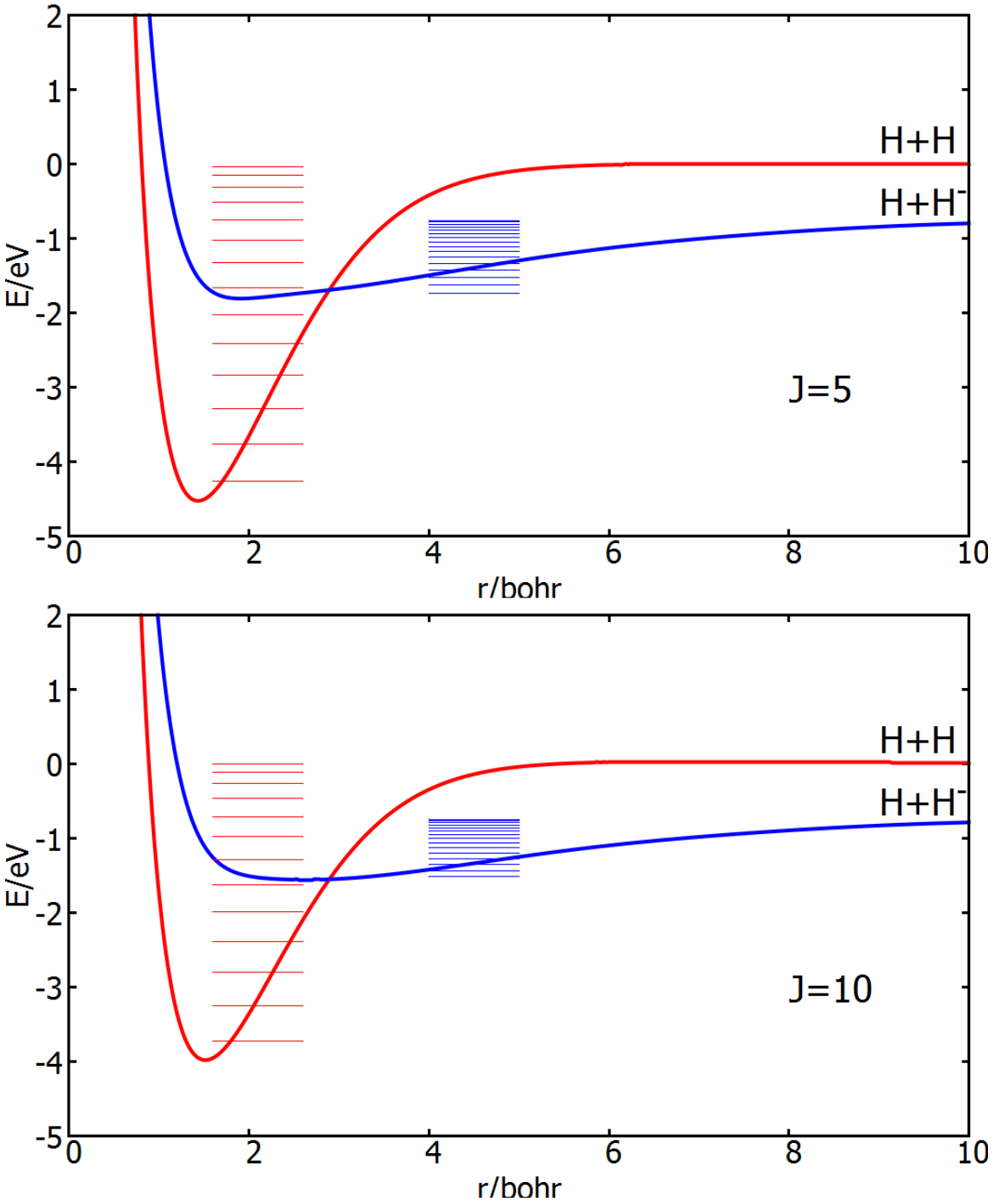

Figure 3.6: Bound states of H_2^- and H_2 calculated for $J = 5$ and 10.

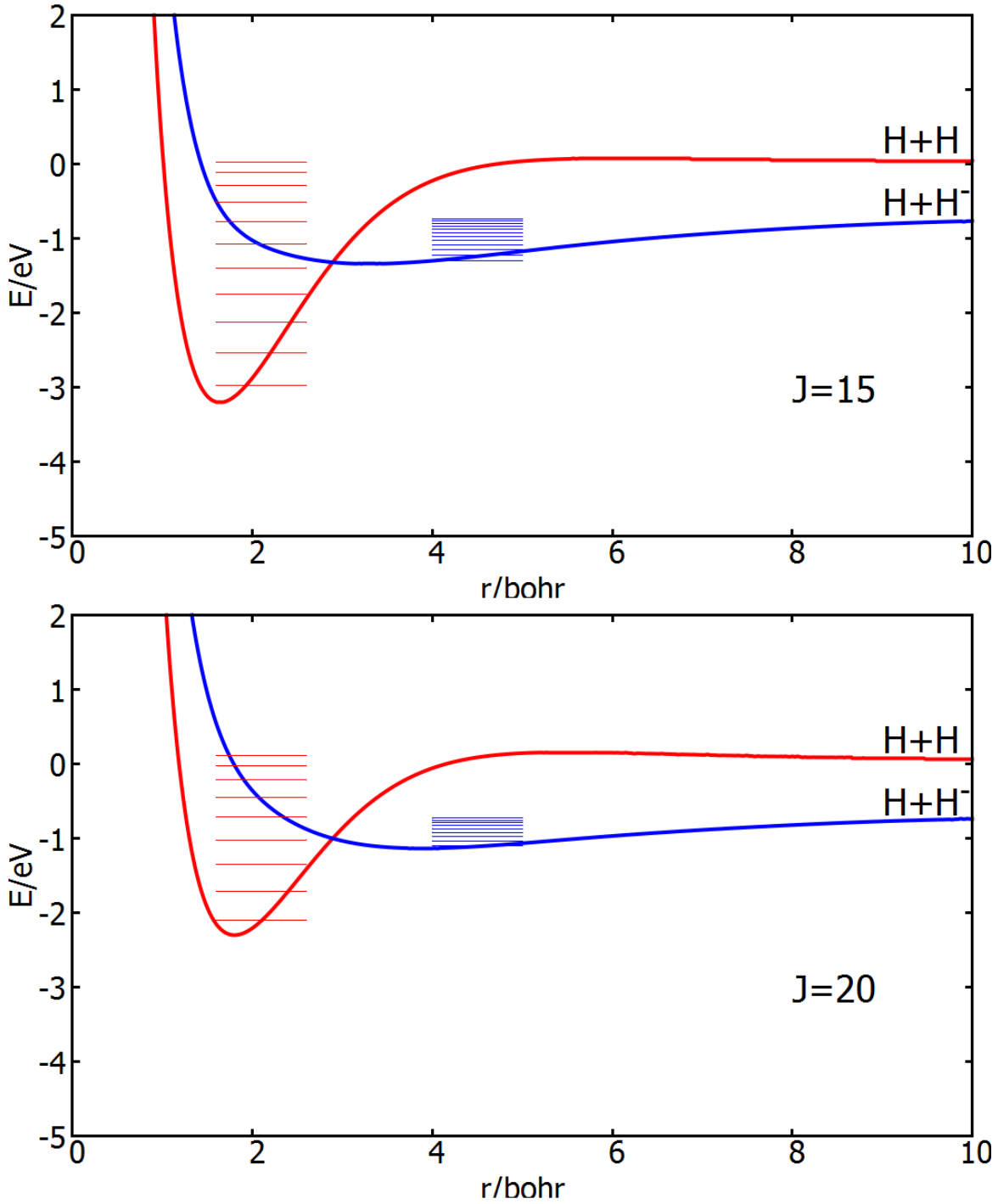

Figure 3.7: Bound states of H_2^- and H_2 calculated for J= 15 and 20.

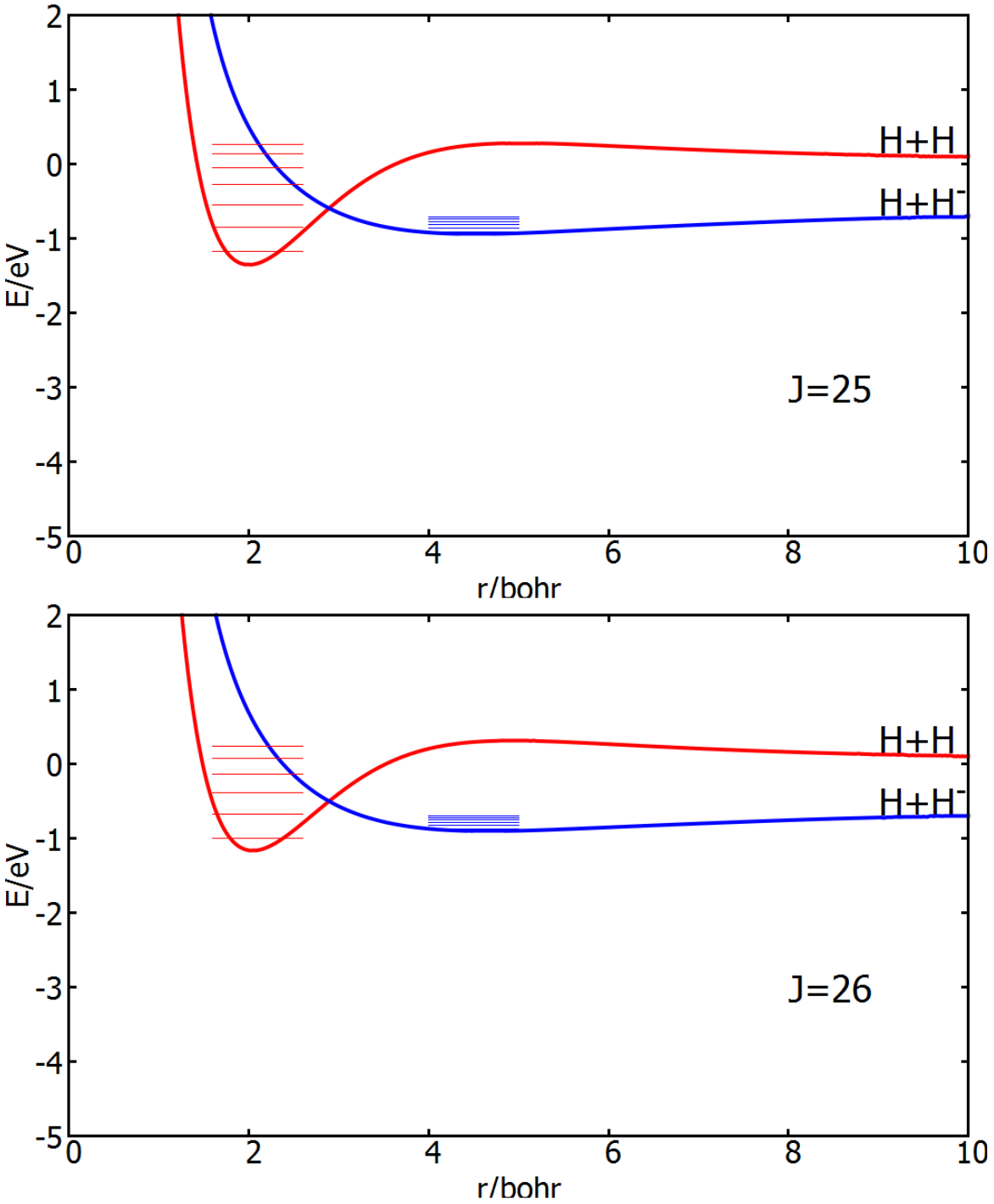

Figure 3.8: Bound states of H_2^- and H_2 calculated for J= 25 and 26.

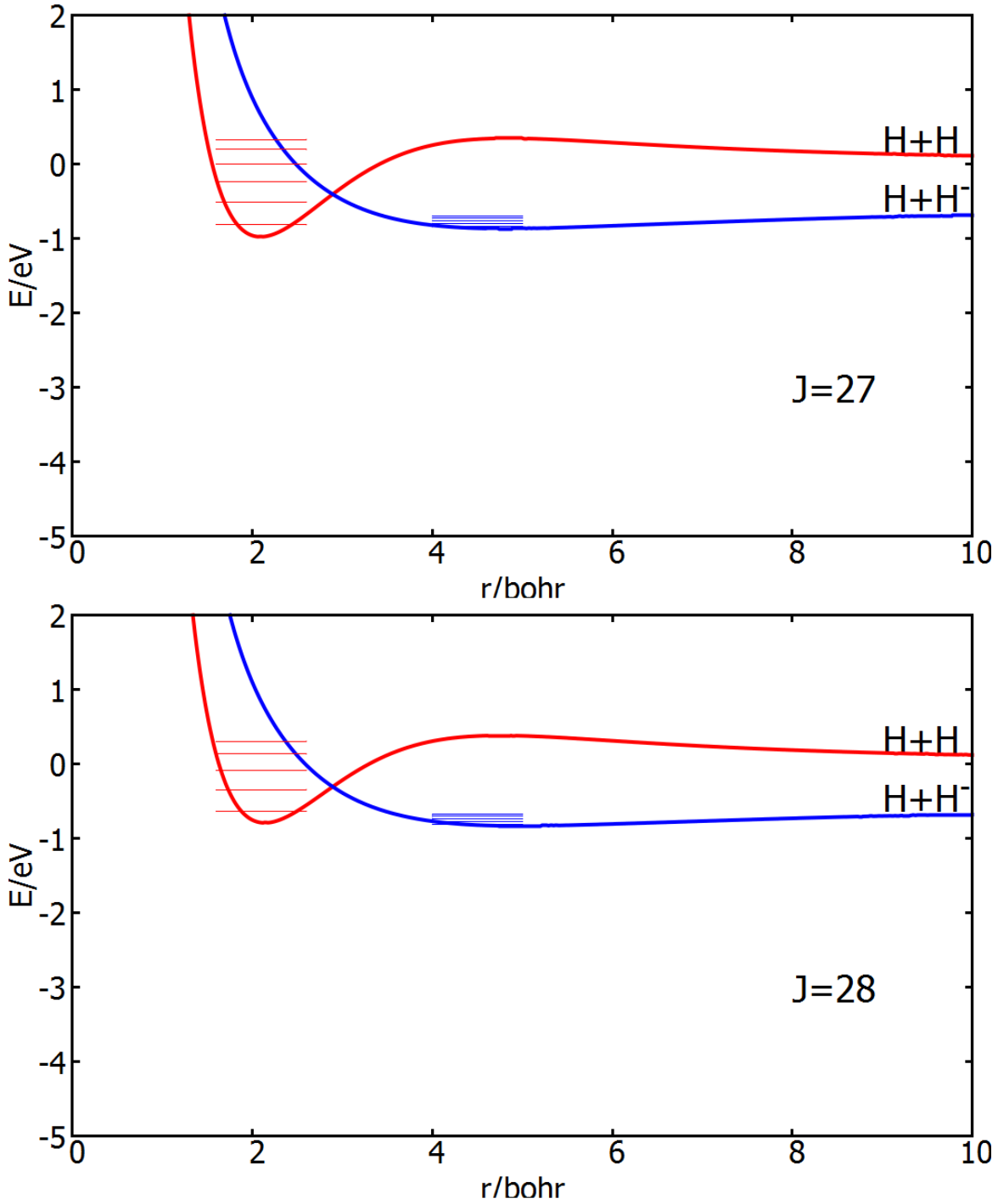

Figure 3.9: Bound states of H_2^- and H_2 calculated for J= 27 and 28.

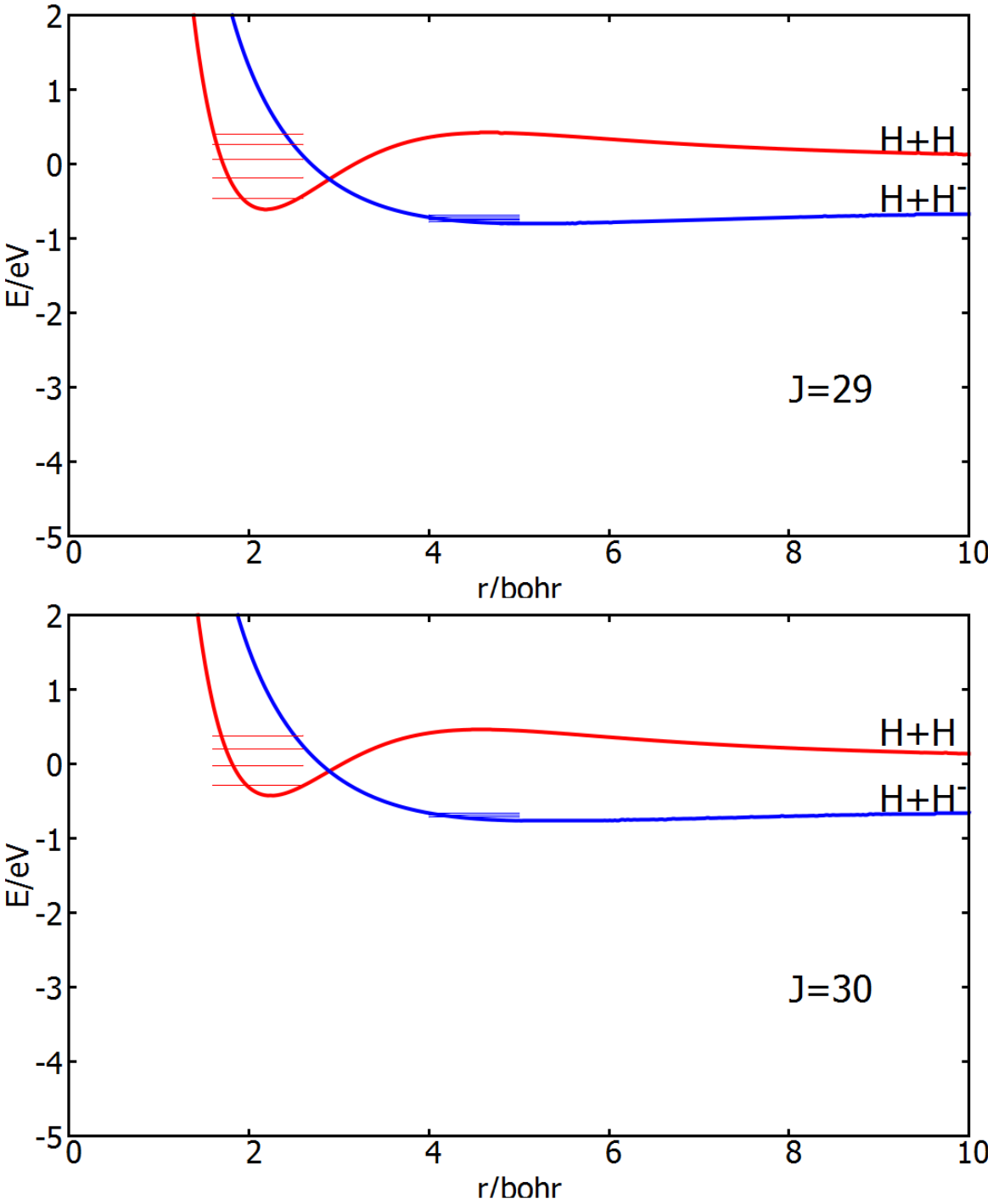

Figure 3.10: Bound states of H_2^- and H_2 calculated for J= 29 and 30.

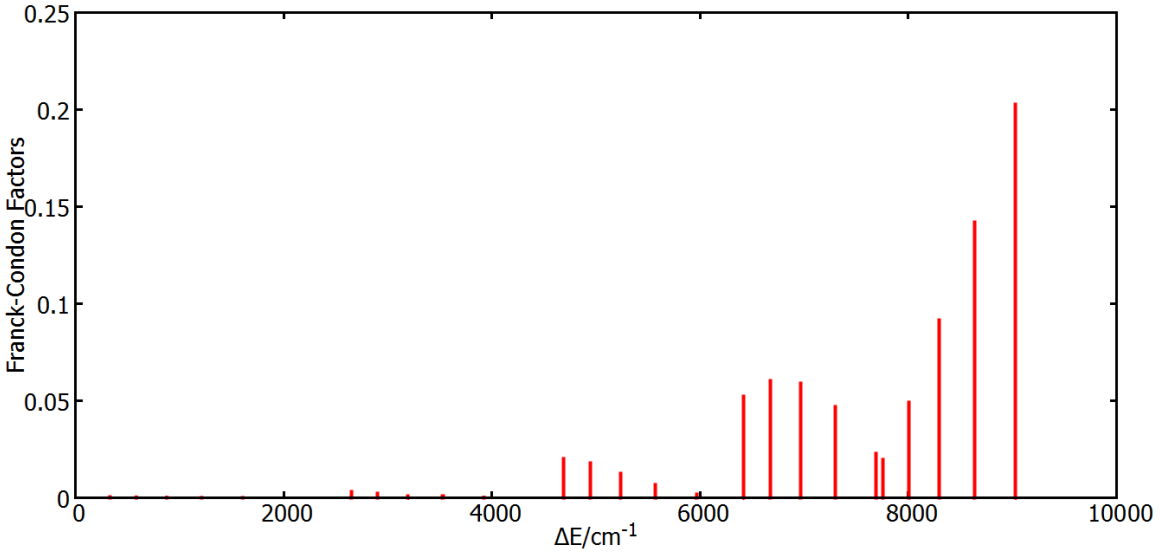

Figure 3.11: Franck-Condon Factors calculated between all vibrational states of J=26 of H_2^- and H_2

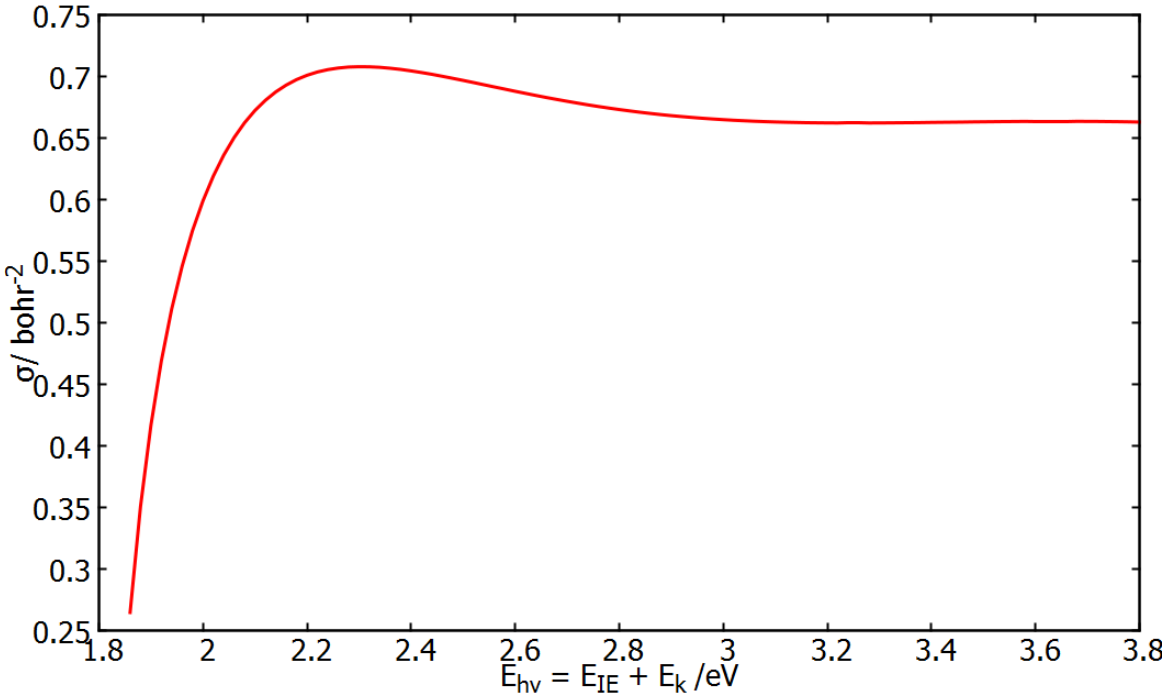

Figure 3.12: The photodetachment cross section of H_2^- plotted as a function of photon energy.

Chapter 4

Appendix

All the computed results of bound and quasibound states of H_2 and H_2^- are reported in Table 4.1 and 4.2. The asymptote is adjusted to correct the electron affinity (0.75eV) of the hydrogen atom.

$v \setminus J$	0	5	10	15	20
0	-1.843463134	-1.733610262	-1.517206787	-1.301811975	-1.099243156
1	-1.707387378	-1.623433564	-1.436432549	-1.225871632	-1.032938221
2	-1.59609677	-1.522668401	-1.354881034	-1.154621739	-0.9723940424
3	-1.493694557	-1.427911113	-1.275505267	-1.088063635	-0.9182854621
4	-1.398676251	-1.339013852	-1.19983296	-1.026652169	-0.8703063331
5	-1.310303209	-1.255916873	-1.128929967	-0.9707170709	-0.8275583115
6	-1.228394454	-1.178876295	-1.06358776	-0.920112761	-0.789480791
7	-1.153126673	-1.108256798	-1.004145812	-0.8743385038	-0.7563824849
8	-1.08466972	-1.044200798	-0.950389165	-0.8330370717	-0.7297596002
9	-1.022872065	-0.9864178692	-0.9017955349	-0.7963659954	
10	-0.9671948602	-0.9343027599	-0.8580008257	-0.7651572641	
11	-0.9169921631	-0.887330409	-0.8191015568	-0.7413560583	
12	-0.8718938893	-0.8453788188	-0.7857615616		
13	-0.832001158	-0.8088386544	-0.7593999055		
14	-0.7979351404	-0.7786797475	-0.7433595347		
15	-0.7709332447	-0.7567190323			
16	-0.7532503568				

$v \setminus J$	26	27	28	29	30
0	-0.8767537346	-0.8427164063	-0.8098010347	-0.7781424	-0.7144659938
1	-0.8278995578	-0.7975561914	-0.7685131042	-0.7408101437	-0.6855768914
2	-0.7863215357	-0.7592730726	-0.7334190086	-0.7088097172	-0.6632403143
3	-0.7500813318	-0.7258956598	-0.7030317529	-0.6818301257	
4	-0.7186694199	-0.6978285041	-0.679451333	-0.7478949333	
5	-0.6940527268				

Table 4.1: Vib-rotational levels of H_2^- in eV units, computed in present work.

$v \setminus J$	0	5	10	15	20
0	-4.477804452	-4.262122027	-3.730418995	-2.975634072	-2.097572359
1	-3.962640257	-3.757873175	-3.253587574	-2.538972777	-1.710139901
2	-3.476293008	-3.282097516	-2.804489116	-2.12941554	-1.350104702
3	-3.01802866	-2.834194834	-2.382884686	-1.747312977	-1.018674305
4	-2.587493382	-2.413947566	-1.988921511	-1.393418203	-0.7175731769
5	-2.184700182	-2.021507464	-1.623126338	-1.068911989	-0.4491993285
6	-1.81002099	-1.657390962	-1.286415972	-0.7754689284	-0.2169581551
7	-1.464190309	-1.32248926	-0.9801342098	-0.515393027	-0.0260772305
8	-1.148326822	-1.018100779	-0.7061294638	-0.2918913477	0.1133672464
9	-0.863981016	-0.7459968905	-0.4669017559	-0.1096901086	
10	-0.6132222502	-0.5085407768	-0.2658854065	0.0230608885	
11	-0.398789347	-0.3088993681	-0.1080611674		
12	-0.2243510755	-0.1514420889	-0.0018119501		
13	-0.094973561	-0.0426094228			
14	-0.0179616476				
15					
16					

$v \setminus J$	26	27	28	29	30
0	-0.9967998309	-0.8156489369	-0.6363513904	-0.4593331664	-0.2850257447
1	-0.6786816692	-0.5104380509	-0.3445845695	-0.1816500552	-0.0222075497
2	-0.3913164834	-0.2371443626	-0.0862010506	0.0607721186	0.2028727592
3	-0.1379696072	0.0002528227	0.1338012554	0.2613433006	0.3806968247
4	0.0763568208	0.1951654221	0.3059071033	0.4031547671	
5	0.2421612799	0.3307321098			

Table 4.2: Vib-rotational levels of H_2 in eV units, computed in present work.

Bibliography

[1] Khvostenko, V. I.; Dukl'skii, V. M. *Sov. Phys. JETP* **1958**, *10*, 465.

[2] Hurley, R. E. *Nucl. Instrum. Methods* **1974**, 307.

[3] Kreckel, H.; Bruhns, H.; Čížek, M.; Glover, S. C. O.; Miller, K. A.; Urbain, X.; Savin, D. W. *Science* **2010**, *329*, 69–71.

[4] Čížek, M.; Horăcek, J.; Domcke, W. *J. Phys. B: At. Mol. Opt. Phys.* **1998**, *31*, 2571.

[5] Kreckel, H.; Herwig, P.; Schwalm, D.; ek, M.; Golser, R.; Heber, O.; Jordon-Thaden, B.; Wolf, A. *J. Phys. : Conf. Series* **2014**, *488*, 012034.

[6] Golser, R.; Gnaser, H.; Kutschera, W.; Priller, A.; Steier, P.; Wallner, A.; Čížek, M.; Horáček, J.; Domcke, W. *Phys. Rev. Lett.* **2005**, *94*, 223003.

[7] Heber, O.; Golser, R.; Gnaser, H.; Berkovits, D.; Toker, Y.; Eritt, M.; Rappaport, M. L.; Zajfman, D. *Phys. Rev. A* **2006**, *73*, 060501.

[8] Čížek, M.; Horáček, J. c. v.; Domcke, W. *Phys. Rev. A* **2007**, *75*, 012507.

[9] Stibbe, D. T.; Tennyson, J. *Chem. Phys. Lett.* **1999**, *308*, 532 – 536.

[10] Srivastava, S.; Sathyamurthy, N.; Varandas, A. *Chem. Phys.* **2012**, *398*, 160 – 167.

[11] Le Roy, R. J. Level 8.2: A Computer Program for Solving the Radial Schrödinger Equation for Bound and Quasibound Levels. 2014; `http://leroy.uwaterloo.ca/programs/`.

[12] Szabo, A.; Ostlund, N. S. *Modern Quantum Chemistry*; Dover Publications, 1989.

[13] Abrol, R.; Sathyamurthy, N.; Harbola, M. K. *Chem. Phys. Lett.* **1999**, *312*, 341 – 345.

[14] Cooley, J. W. *Mathematics of Computation* **1961**, *15*, 363–374.

[15] Young, P. Numerov method for integrating the one-dimensional Schrödinger equation. 2009; `physics.ucsc.edu/~peter/242/numerov.pdf`.

[16] Simons, J. In *Response Theory and Molecular Properties*; Jensen, H., Ed.; Advances in Quantum Chemistry; Academic Press, 2005; Vol. 50; pp 213 – 233.

[17] Krylov, A. I. *Ann. Rev. Phys. Chem.* **2008**, *59*, 433–462.

[18] Melania Oana, C.; Krylov, A. I. *J. Chem. Phys.* **2007**, *127*.

[19] Rudnev, V.; Ureña, A. G. *Review of Scientific Instruments* **2013**, *84*.

[20] Rudnev, V.; Schlösser, M.; Telle, H. H.; Ángel González Ureña, *Chem. Phys. Lett.* **2015**, *639*, 41 – 46.

[21] Barca, G. M. J.; Gilbert, A. T. B.; Gill, P. M. W. *J. Chem. Phys.* **2014**, *141*.

[22] Gozem, S.; Krylov, A. I. ezDyson. `http://iopenshell.usc.edu/downloads/ezdyson`.